JAEA-Research
2014-015

Preliminary Conceptual Design of the Secondary Sodium Circuit-eliminated JSFR (Japan Sodium Fast Reactor) Adopting a Supercritical CO_2 Turbine System (1)
- Sodium/CO_2 Heat Exchanger -

Naoyuki KISOHARA, Yoshihiko SAKAMOTO and Shoji KOTAKE

JSFR Systems Development Planning Office
Advanced Nuclear System Research and Development Directorate

September 2014
Japan Atomic Energy Agency
日本原子力研究開発機構

JAEA-Research

JAEA-Research 2014-015

Preliminary Conceptual Design of the Secondary Sodium Circuit-eliminated JSFR (Japan Sodium Fast Reactor) Adopting a Supercritical CO_2 Turbine System (1) - Sodium/CO_2 Heat Exchanger -

Naoyuki KISOHARA, Yoshihiko SAKAMOTO[+1] and Shoji KOTAKE[*1]

JSFR Systems Development Planning Office
Advanced Nuclear System Research and Development Directorate※
Japan Atomic Energy Agency
Oarai-machi, Higashiibaraki-gun, Ibaraki-ken

(Received June 16, 2014)

Research and development of the supercritical CO_2 (S-CO_2) cycle turbine system is underway in various countries for further improvement of the safety and economy of sodium-cooled fast reactors. The Component Design and Balance-Of-Plant (CD&BOP) of the Generation IV International Nuclear Forum (Gen-IV) has addressed this study, and their analytical and experimental results have been discussed between the relevant countries.

JAEA, who is a member of the CD&BOP, has performed a design study of an S-CO_2 gas turbine system applied to the Japan Sodium-cooled Fast Reactor (JSFR). In this study, the S-CO_2 cycle turbine system was directly connected to the primary sodium system of the JSFR to eliminate the secondary sodium circuit, aiming for further economical improvement. This is because there is no risk of sodium-water reaction in the S-CO_2 cycle turbine system of SFRs.

The Na/CO_2 heat exchanger is one of the key components for the secondary sodium system eliminated SFR, and this report describes its structure and the safety in case of CO_2 leak. A Printed Circuit Heat Exchanger (PCHE), which has a greater heat transfer performance, is employed to the heat exchanger. Another advantage of the PCHE is to limit the area affected by a leak of CO_2 because of its partitioned flow path structure. A SiC/SiC ceramic composite material is used for the PCHE to prevent crack growth and to reduce thermal stress.

The Na/CO_2 heat exchanger has been designed in such a way that a number of small heat transfer modules are combined in the vessel in consideration of manufacture and repair. The primary sodium pump is installed in the center of the heat exchanger vessel. CO_2 leak events in the heat exchanger have been also evaluated, and it revealed that no significant effect has arisen on the core or the primary sodium boundary.

Keywords : Secondary Sodium Circuit Elimination, JSFR, Supercritical CO_2, Sodium/CO_2 Heat Exchanger

---

※ Fast Reactor Cycle System Design and Standard Development Office, Advanced Fast Reactor Cycle System Research and Development from April 1st 2014.

+1 Project Promotion Office

＊1 The Japan Atomic Power Company

超臨界炭酸ガスタービンシステムを採用した2次系削除 JSFR（Japan Sodium Fast Reactor）の概念検討（1） –ナトリウム／炭酸ガス熱交換器–

日本原子力研究開発機構
次世代原子力システム研究開発部門※
炉システム開発計画室

木曽原 直之、阪本 善彦+1、小竹 庄司*1

（2014 年 6 月 16 日受理）

ナトリウム冷却高速炉の安全性と経済性の更なる向上のために超臨界炭酸ガスサイクルタービンシステムの研究開発が世界各国で進められている。第4世代国際原子力システムフォーラム(Gen-IV)／機器設計及びバランス・オブ・プラント(CD&BOP)もこの研究テーマを取り扱い、これまで関係国間で議論されてきている。

原子力機構は CD&BOP のメンバーの一員でもあり、超臨界炭酸ガスタービンシステムの JSFR への適用性を検討してきた。本検討では、超臨界炭酸ガスタービンシステムを1次ナトリウム系に直結し、2 次系削除型 JSFR として、将来の更なる経済性向上を狙った。なぜなら、超臨界炭酸ガスタービンシステムは SFR においてはナトリウム／水反応がないからである。

ナトリウム／炭酸ガス熱交換器はこの 2 次系削除型 JSFR にとって重要機器の一つであり、本報告書ではその構造や炭酸ガスリーク時の安全性に関して述べる。ナトリウム／炭酸ガス熱交換器では、伝熱性能に優れた PCHE とした。もう一つの PCHE の特長は、流路が区画されていることから、炭酸ガスリークが発生しても、その影響範囲を限定できることである。また、き裂進展防止と熱膨張低減のために SiC/SiC セラミック複合材料を PCHE の材料に用いた。

ナトリウム／炭酸ガス熱交換器は、製作性や補修性を考慮して、多数の小型の熱交換モジュールを、熱交換容器の中で組み合わせる構成とした。熱交換器容器の中央部には 1 次系ポンプを配置した。熱交換器における炭酸ガスリークも評価し、この結果、炉心や 1 次ナトリウムバウンダリへの影響は無いことが判った。

大洗研究開発センター(駐在)：〒311-1393 茨城県東茨城郡大洗町成田町 4002
※ 次世代高速炉サイクル研究開発センター　設計・規格基準室（2014 年 4 月 1 日改組）
+1 プロジェクト推進室
*1 日本原子力発電株式会社

Contents

目次

[Table list]

[Figure list]

This is a blank page.

1. Introduction

The sodium-cooled fast reactor (SFR) that is being developed by the Japan Atomic Energy Agency (JAEA) is a loop-type reactor. One of the advantages of the loop-type reactor is the possibility of eliminating the secondary sodium system. For the reason, a design study of the secondary sodium circuit-eliminated JFSR was conducted to evaluate its technical feasibility and the effect of reducing the volume as an option for JSFR systems for the future commercialization phase.

Important conditions for the elimination of the secondary sodium circuit are no risk of sodium-water reactions and greatly reduced impact on the primary sodium system and the reactor core in case of heat exchanger failure. To meet these conditions, a conceptual design study of the secondary sodium circuit-eliminated JSFR was conducted employing a supercritical CO_2 turbine system and a Na/CO_2 PCHE (printed circuit heat exchanger).

In this study, the 1,500 MWe JSFR with the secondary sodium circuit and the steam turbine was used as the base reactor concept. A preliminary design study of the supercritical CO_2 gas cycle system and Na/CO_2 heat exchanger suitable for the reference JSFR was conducted. The other specifications, such as the reactor structure, 2-loop cooling system configuration, decay heat removal system, plant thermal power and the primary system heat balance, were set as the same as those of the reference JSFR.

This report describes the Na/CO_2 heat exchanger, which is the key component to the elimination of the secondary sodium circuit. A structural concept of the Na/CO_2 heat exchanger suitable for the primary sodium system was determined in consideration of the safety, heat exchange performance, manufacturability, and repairability. A preliminary safety evaluation in case of CO_2 leak was also carried out.

2. Overview of secondary sodium circuit-eliminated JFSR

A supercritical CO_2 gas cycle and a PCHE-type Na/CO_2 heat exchanger were employed in the study of the secondary sodium circuit-eliminated JFSR. In addition, a SiC/SiC ceramic composite material was used for the Na/CO_2 heat exchanger (PCHE) to prevent a crack initiation and its growth. Although both the supercritical CO_2 gas turbine system and the PCHE are technologies under development, this study was conducted on the premise of the adoption of these technologies. The advantages of these technologies are described in (1) through (3) below;

2.1 Supercritical CO_2 gas turbine system

A configuration diagram of the supercritical CO_2 gas turbine system is shown in Fig. 2.1 with a conventional steam Rankin system. A high cycle thermal efficiency can be achieved because the compression of CO_2 gas in the supercritical region significantly reduces loss in the compressor. Also, the CO_2 gas turbine system is smaller and more simply configured compared with the steam turbine system, allowing for a reduction in the system dimension.

Applying the supercritical CO_2 gas cycle system to a sodium-cooled fast reactor requires Na/CO_2 heat exchangers. Even in the case that the heat exchanger fails and sodium-CO_2 reaction occurs, reaction products are Na_2CO_3 (solid) and CO; and there is no production of flammable gas (H_2) or strongly-alkaline corrosion product (NaOH) produced by the sodium-water reaction. Furthermore, the solid reaction product, Na_2CO_3, suppresses the progress of the sodium-CO_2 reaction. From these features, the sodium-CO_2 reaction is much milder than the sodium-water reaction in steam generators.

As described above, the safety of Na/CO_2 heat exchanger in the supercritical CO_2 gas turbine system can be dramatically improved compared with that of the conventional the steam turbine system.

2.2 PCHE (Printed Circuit Heat Exchanger)

A structural concept of the PCHE is shown in Fig. 2.2. This heat exchanger differs from the shell & tube heat exchanger that has been previously used in FBRs (Fig. 2.3). In a PCHE, the heating fluid (sodium) and the heated fluid (CO_2) flow in the reverse direction and their flow path are alternately arranged. The flow paths are partitioned by walls. Since the

PCHE has a large heat transfer area per unit volume, it is suitable for a gas with a low heat transfer coefficient.

The advantage of the PCHE is the capability of limiting the area affected by CO_2 leak resulting from a failure of the flow path because the flow paths are partitioned. In shell & tube heat exchangers, a reaction jet caused by one tube failure will affect many adjacent tubes, as illustrated in Fig. 2.3. However, in the PCHE, the influence of CO_2 leak is limited within one flow path, at least in the initial phase, as shown in Fig. 2.2.

Manufacturing a PCHE in a large-scale, however, is impractical. Accordingly, it is necessary to manufacture it as small-scale heat transfer modules and combine them in a heat exchanger vessel to form the flow paths.

2.3 SiC/SiC composite material for PCHE

The SiC/SiC ceramic composite material is based on silicon carbide ceramics using a silicon carbide fiber as reinforcement. Because of its pseudo-ductility, excellent high-temperature strength and low thermal expansion coefficient, this material is advantageous for a heat exchanger, in which hot-leg (sodium side) and cold-leg (CO_2 side) flow paths are incorporated together, from a structural integrity perspective.

Furthermore, it is possible to provide a crack arresting layer between the sodium and CO_2 flow paths in its manufacturing process. This would provide a mechanism to prevent through leaks.

This report describes the design of the supercritical CO_2 gas turbine system in (1) above. Other results are the estimated dimensions of the secondary sodium circuit-eliminated JSFR and the comparison of the building volume between plants with and without the secondary sodium circuit.

The conditions of the primary sodium system assumed for this study are the same as those of the reference 1500 MWe JSFR, as described below:

- Reactor thermal power: 3530 MWth
- Number of the primary sodium loops: 2
- Primary sodium flow rate: 3.24×10^7 kg/hr/loop
- Reactor outlet sodium temperature: 550°C
- Reactor inlet sodium temperature: 395°C

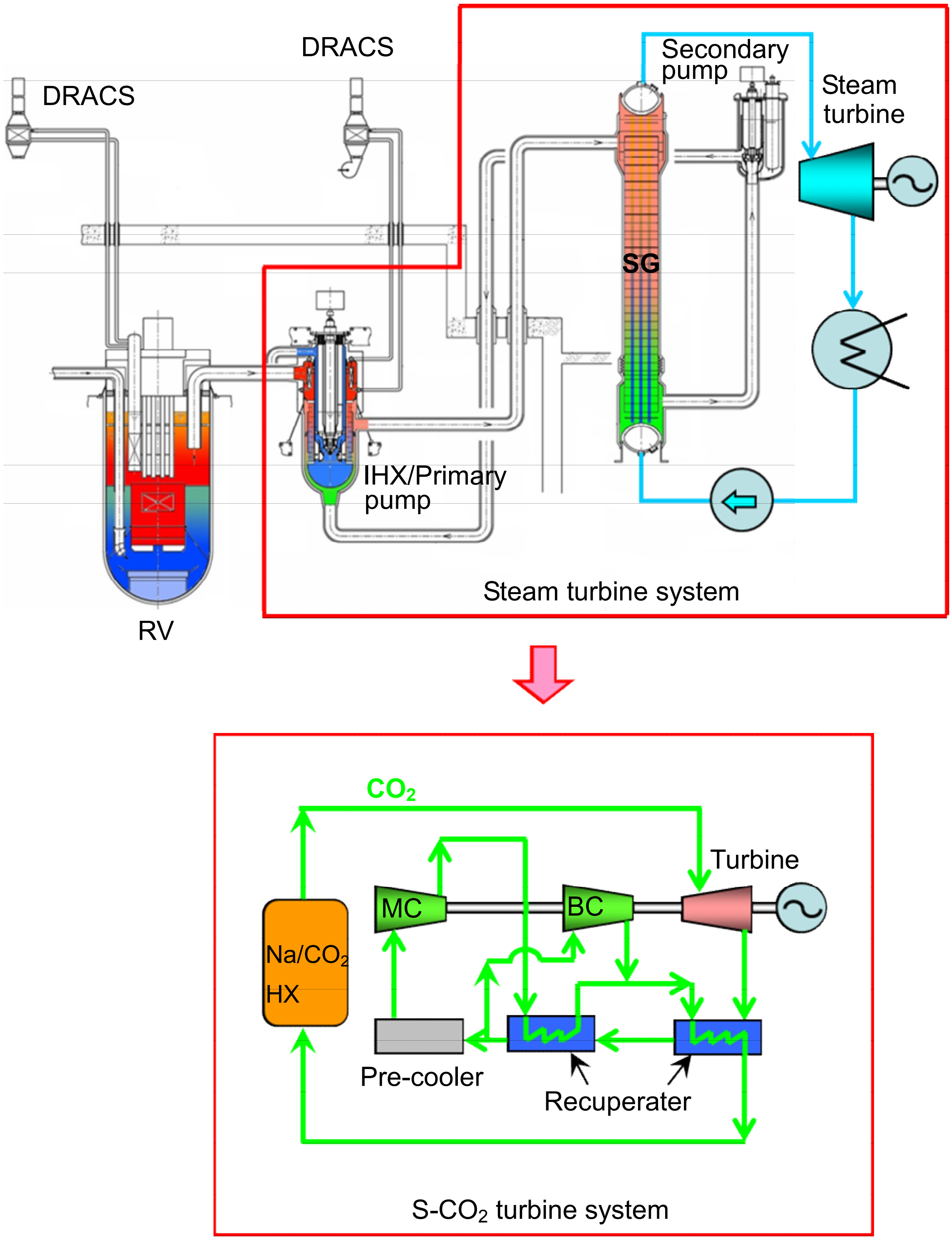

Fig. 2.1 Supercritical CO_2 turbine system

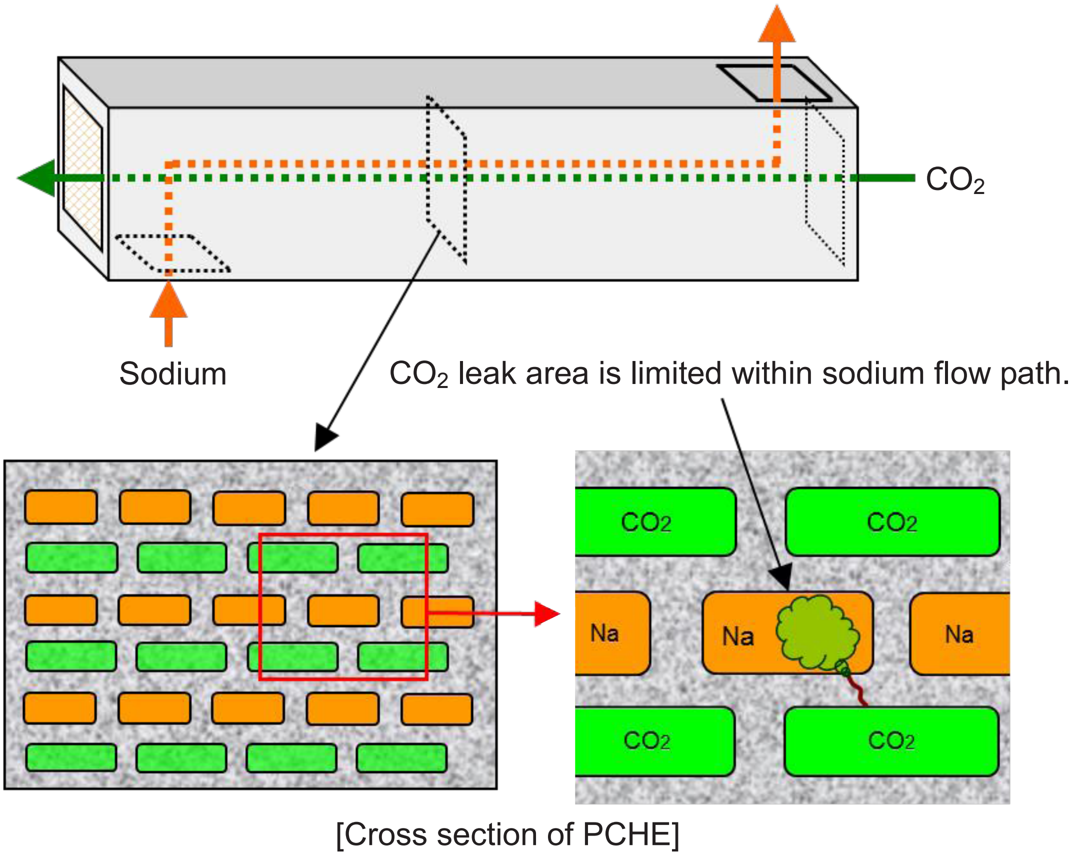

Fig. 2.2 Printed circuit heat exchanger (PCHE)

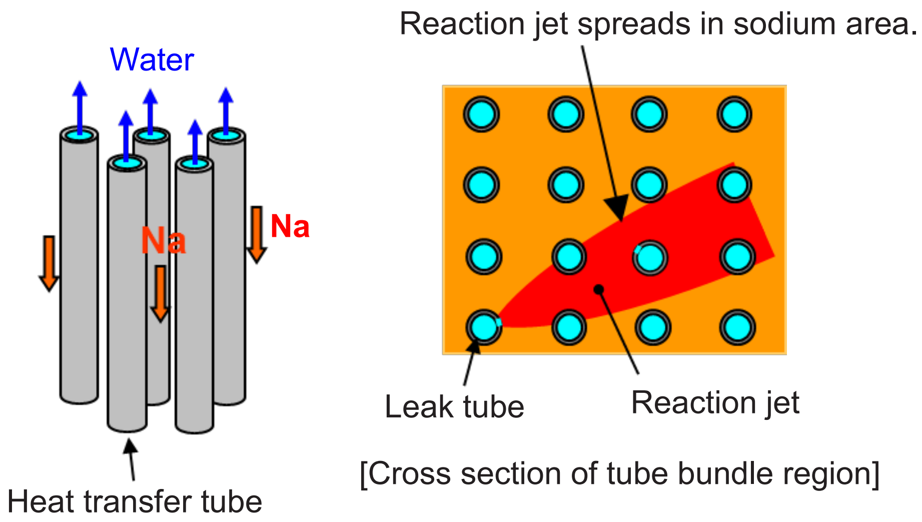

Fig. 2.3 Shell and tube type heat exchanger

3. Na/CO_2 heat exchanger

3.1 Configuration of heat exchanger unit

The configuration of the Na/CO_2 PCHE (Printed circuit heat exchanger) is shown in Fig. 3.1. Since the PCHE has a layered configuration in which sodium and CO_2 flow paths are arranged one after the other, it is impossible to provide the inlet/outlet of the sodium and CO_2 flow paths on the same side surface. The inlet/outlet of sodium is separated from those of CO_2 by arranging the sodium flow paths in the form of a crank.

Figure 3.2 shows the configuration of the PCHE in which the CO_2 inlet/outlet pipe is installed. The CO_2 inlet/outlet piping has a double-walled configuration consisting of inner and outer pipes. The A-A and B-B cross sections show the CO_2 and sodium flow paths, respectively. The right-side CO_2 pipe is the inlet side through which CO_2 flows into the heat exchange region, toward the left direction of the PCHE. The CO_2 that has exchanged heat with sodium flows out to the left-side CO_2 pipe and then flows upward.

No sodium pipe is connected to the PCHE. This is because the PCHE is contained in the heat exchanger vessel and immersed in sodium, which flows outside of the PCHE. (Details are given in Section 3.3.)

In manufacturing the Na/CO_2 heat exchanger, small heat transfer modules (PCHE modules) are fabricated first as shown in the left illustration of Fig. 3.3. These heat transfer modules are then longitudinally layered to form a heat exchanger unit (PCHE unit). The heat exchanger units are circumferentially arranged and connected in the heat exchanger vessel to form the sodium and CO_2 flow paths.

3.2 Sizing of heat exchanger unit

The heat transfer area of the heat transfer module was obtained by the configuration of heat exchanger, heat transfer coefficients of fluids, and thermal conductivity of the heat exchanger material (SiC/SiC composite material).

The shape and specifications of the CO_2-side flow path are listed in Table 3.1. The S-fin type flow path is employed for the CO_2-side to reduce the flow resistance and enhance the heat transfer coefficient. The S-fin type flow path has the advantage of low pressure loss compared with the Zigzag type flow path, although both types have similar heat transfer performance.

The straight flow path is employed for the sodium-side, as shown in Fig.

3.4. This flow path is partitioned, meaning that the area of leak will be restricted in case of a CO_2 leak. Although the straight flow path has lower heat transfer performance compared with the S-fin type flow path, since sodium has an excellent heat transfer coefficient, even the straight flow path can achieve a sufficient heat transfer coefficient.

The specifications of plate thickness, flow path height, fin thickness and the minimum thickness were set to be the same as those of the CO_2-side flow path; and the flow path width was set to be equivalent to the maximum width of the S-fin type flow path.

The heat transfer area of the heat transfer module was calculated based on the required conditions of the Na/CO_2 heat exchanger, which are described below, to determine the dimensions (sizing).

- Inlet CO_2 temperature (°C): 385.8
- Outlet CO_2 temperature (°C): 527
- Inlet sodium temperature (°C): 550
- Outlet sodium temperature (°C): 395
- CO_2 flow rate (kg/s): 20,245
- Sodium flow rate (kg/s): 18,000
- Heat exchange capacity (kJ/s): 3,530,000
- Allowable sodium-side pressure loss (MPa): 0.0217
- CO_2 pressure loss ratio (%): 2*

(* The pressure loss ratio estimation includes the connecting piping.)

The following equations are used for the heat transfer calculation of CO_2 and sodium-side flow paths, respectively.

[CO_2 side]

- Nusselt number: $Nu = 0.1043Re^{0.658}$
- Coefficient of friction: $f = 3.288Re^{-0.361}$

[Sodium side]

- Nusselt number: $Nu = 0.023Re^{0.8}Pr^{0.4}$ (Dittus-Boelter equation)

Since the sodium-side flow path is in the form of a crank, cross-flow heat exchange occurs at the inlet/outlet portions, and counter-flow heat exchange occurs in the other areas. Both the heat exchange modes were taken into account in calculating the heat transfer area of the heat transfer module.

The thermal conductivity of SiC/SiC composite material was set to be 25 W/(m·K) for the heat transfer calculation, and the length of the heat transfer area was determined to keep the pressure loss no greater than the allowable value in consideration of the manufacturability of SiC/SiC composite material (limitation of the size).

The specifications and configuration of one heat transfer module obtained based on the heat transfer calculation are shown in Fig. 3.5. The dimensions of the heat transfer module are 750 mm in length, 202 mm in height and 230 mm in width. There are 60 layers of sodium flow paths and 60 layers of CO_2 flow paths one after the other in the heat exchange module, and the heat exchange capacity is 817 kWth/module. The pressure losses were calculated to be 0.0166 MPa on the sodium side and 0.242 MPa on the CO_2 side; and both values meet the design requirements.

3.3 Structural concept of heat exchanger

3.3.1 Layout of heat exchanger units

The layout of the combined heat transfer modules in the heat exchanger vessel is shown in Figs. 3.6 and 3.7. Sixty heat transfer modules (202mm × 230mm × 750mm) are piled up to form one heat exchanger unit. The dimension of this heat exchanger unit including the CO_2 inlet outlet piping is 12.2 m high, 0.3 m wide and 1.33 m long. The heat exchange capacity of one heat exchanger unit is 49.0 MWth/unit. Thirty eight heat exchanger units are circumferentially arranged in the vessel as shown in the lower right of Fig. 3.6. Thirty six heat exchanger units were sufficient to achieve the specified heat exchange capacity; however, two more units were installed as spare units.

As the circumferential arrangement of the heat exchanger units makes space in the central area of the vessel, the pump is installed here. The heat transfer tubes of the PRACS are arranged in the sodium main flow path of the hot-leg side between the heat exchanger units.

3.3.2 Sodium flow path

The whole heat exchanger units are immersed in sodium in the heat exchanger vessel. The outer and inner regions inside the heat exchanger vessel are arranged for hot-leg and cold-leg sodium, respectively, as shown in the horizontal cross section of the upper right section of Fig. 3.6. Sodium flows from the outer to inner regions in the heat exchanger unit. This is because the pump was installed in the central area of the heat exchanger and, accordingly, it is appropriate to maintain low temperatures by arranging the cold-leg in the inner region. The sodium exchanging heat with CO_2 in the unit flows out to the cold-leg plenum, flows downward, and then changes its flow direction upward at the bottom to enter the pump.

3.3.3 CO_2 flow path

The CO_2 inlet/outlet piping of the heat exchanger unit is connected to the CO_2 ring header above the heat exchanger. The CO_2 supplied from the CO_2 ring header flows downward through the CO_2 inlet piping and enters the heat exchanger unit. The CO_2 flows from the inner to outer sides in the heat exchanger unit so that the CO_2 and sodium counter-flow. Then, the CO_2 flows upward through the CO_2 outlet piping and enters the CO_2 outlet ring header.

3.3.4 Main sodium piping

There are 3 main primary sodium pipings between the R/V and the heat exchanger vessel: 2 of these are on the hot-leg side and the remaining one is on the cold-leg side. Two sets of reduced diameter piping are used for the hot-leg to shorten the length of the heat exchanger. The cold-leg sodium piping is placed horizontally from the outlet of the pump. For this reason, the CO_2 inlet/outlet vertical piping cannot be placed in the cold-leg sodium piping area: that is, the heat exchanger unit cannot be placed immediately below the cold-leg sodium piping, leaving this area empty. Therefore, a single cold-leg piping was employed to minimize the empty space in the vessel.

3.3.5 Repair

If a CO_2 leak occurs in a PCHE unit, it is impossible to gain access to the flow path of the unit and to repair it by flow path plugging. In this case, in-place plugging method is applied to the entire unit. Accordingly, 2 extra heat exchanger units are installed in the heat exchanger vessel assuming plugging for the margin.

A failed heat exchanger unit is not replaced by a new one. This is due to the difficulty of welding and reconnecting the piping for replacement unit because this heat exchanger is a primary component. Another reason is that the pump support structure poses an impediment to the upward extraction of a failed heat exchanger unit.

3.3.6 Cover gas structure

The heat exchanger was designed to have a space filled with a cover gas. A bellows on the sodium boundary is necessary to absorb the thermal expansion difference between the heat exchanger vessel and heat exchanger unit. Installing the bellows in the cover gas volume can reduce the possibility of its failure.

Detection of CO_2 leaking into sodium in the heat exchanger is also required for safety. It is impossible to detect CO_2 by means of permeation through a nickel membrane in sodium as is possible in hydrogen detection. Accordingly, the cover gas volume is needed for gas chromatography detection of CO_2 released from sodium. The cover gas volume of the heat exchanger has another advantage to moderate the pressure rise in case of a large leak.

The dimensions of the heat exchanger vessel was estimated based on the above heat transfer calculation and structural consideration. The dimensions are an outer diameter of 8.6 m and a height of 20.1 m (excluding the pump area).

3.4 Comparison of size with shell & tube heat exchanger

The heat transfer area and the volume of heat exchange region between the Na/CO_2 HX, Na/Na HX and the double-walled tube steam generator (SG) are compared in Table 3.2.

The Na/CO_2 heat exchanger requires large heat transfer area due to inferior heat transfer property on the gas side. The heat transfer area of the Na/CO_2 heat exchanger is approx. 6 times that of the Na/Na HX and approx. twice that of the SG.

However, since the PCHE has a greater heat transfer area per unit volume of the heat exchange region, the volume of heat exchange region of the PCHE is approx. 1.2 times that of the IHX and approx. 1/5 of that of the SG.

Thirty-eight PCHE modules need to be arranged in the heat exchanger vessel in the consideration of the sodium flow space. And also, because no PCHE unit is installed immediately below the sodium cold-leg piping, empty space appears here. Due to these reasons, the vessel of the Na/CO_2 heat exchanger (HX) is larger than that of the Na/Na HX and SG in spite of its small hear transfer area. Figure 3.8 shows the comparison of the sizes of these heat exchangers. The size of the vessel of the Na/CO_2 HX is approx. 3.6 times and 2.4 times that of the Na/Na HX and SG, respectively.

Table 3.1 CO_2 flow path of heat transfer module

Item	Side	S-fin type
Fin configuration	Cold/Hot	
Plate thickness, mm	Cold/Hot	1.5
Channel depth, mm	Cold/Hot	0.94
Wall thickness, mm	Cold/Hot	0.54
Channel width, mm	Cold/Hot	1.31
Fin thickness, mm	Cold/Hot	0.8
Hydraulic diameter, mm	Cold/Hot	1.09[a)]
Bending angle, °	Cold/Hot	76
Pitch in *x*-direction /*y*-direction, mm	Cold/Hot	7.565/3.426
Number of plates	Cold	4
	Hot	8
Number of fluid channels	Cold	44
	Hot	96
MCHE dimensions H/W/D, mm	-	745.2/76/29
Heat transfer area, m^2	Cold	0.2559
	Hot	0.5099
Free flow area, m^2	Cold	5.42×10^{-5}
	Hot	11.82×10^{-5}

[a)] Defined using a minimal free flow area.

Table 3.2 Comparison of heat transfer area

	S-CO_2 Brayton cycle JSFR (Secondary sodium circuit elimination system)		Steam Rankin cycle JSFR (Reference)	
Heat Transfer area (m^2)	Na/CO_2 heat exchanger	28080 m^2	IHX (Na/Na HX) SG (Na/Water HX)	4480 m^2 13850 m^2 (Total 18330m^2)
Volume of heat transfer region (m^3)	Na/CO_2 heat exchanger	65.2 m^3	IHX (Na/Na HX) SG (Na/Water HX)	52.9 m^2 333.9 m^2 (Total 386.8m^2)

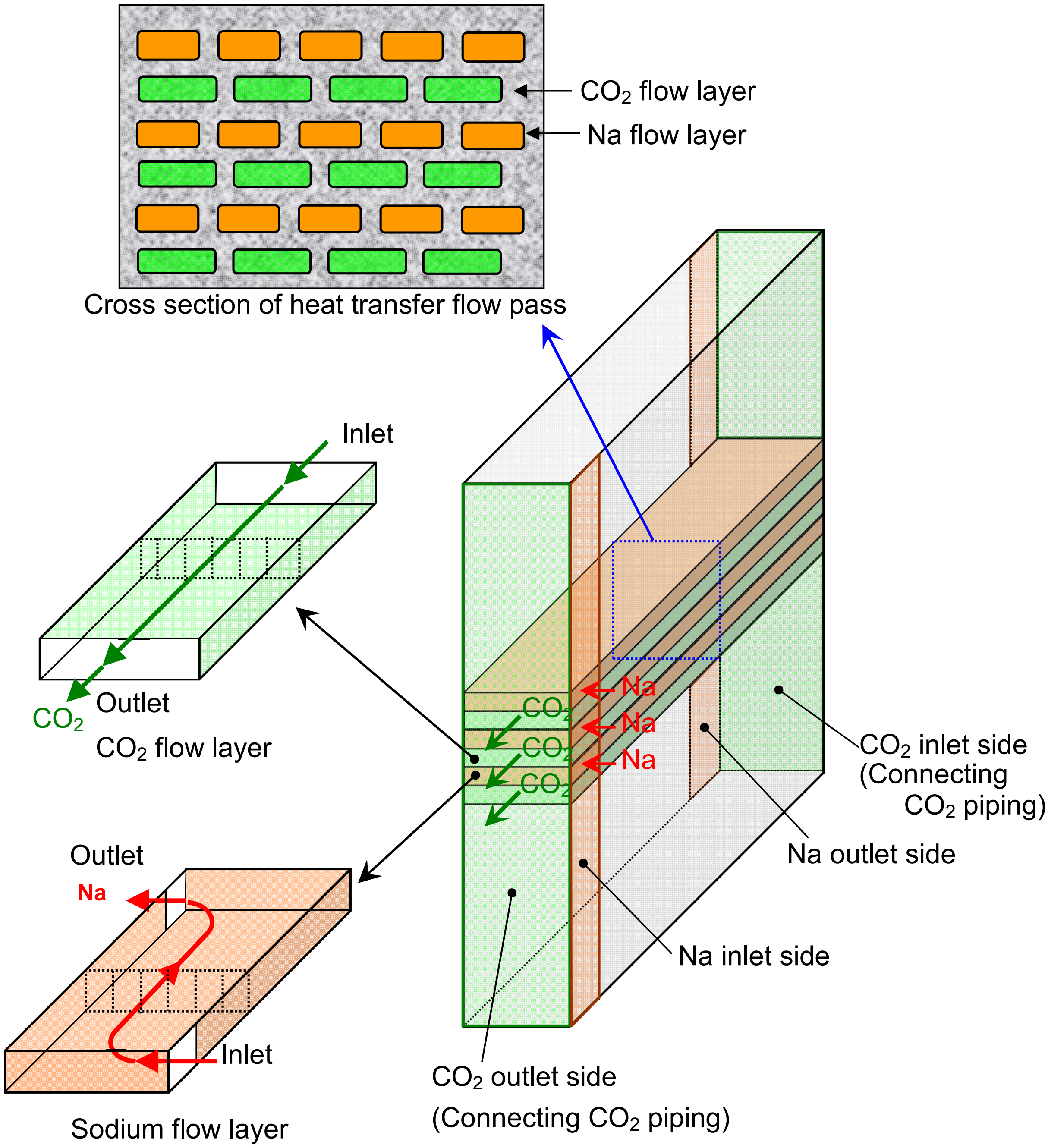

Fig. 3.1 Na/CO_2 PCHE

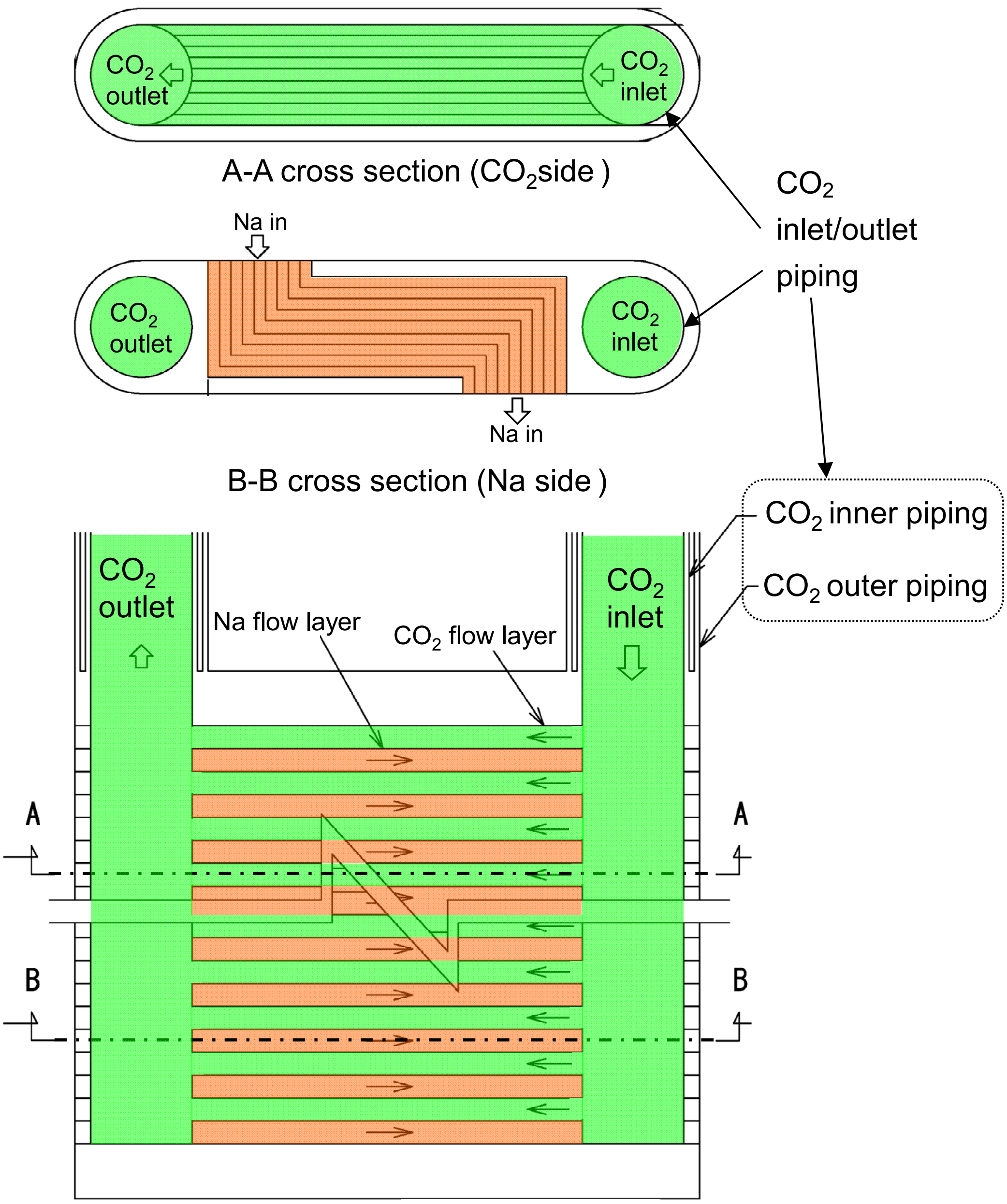

Fig. 3.2 Na/CO_2 PCHE with CO_2 inlet/outlet piping

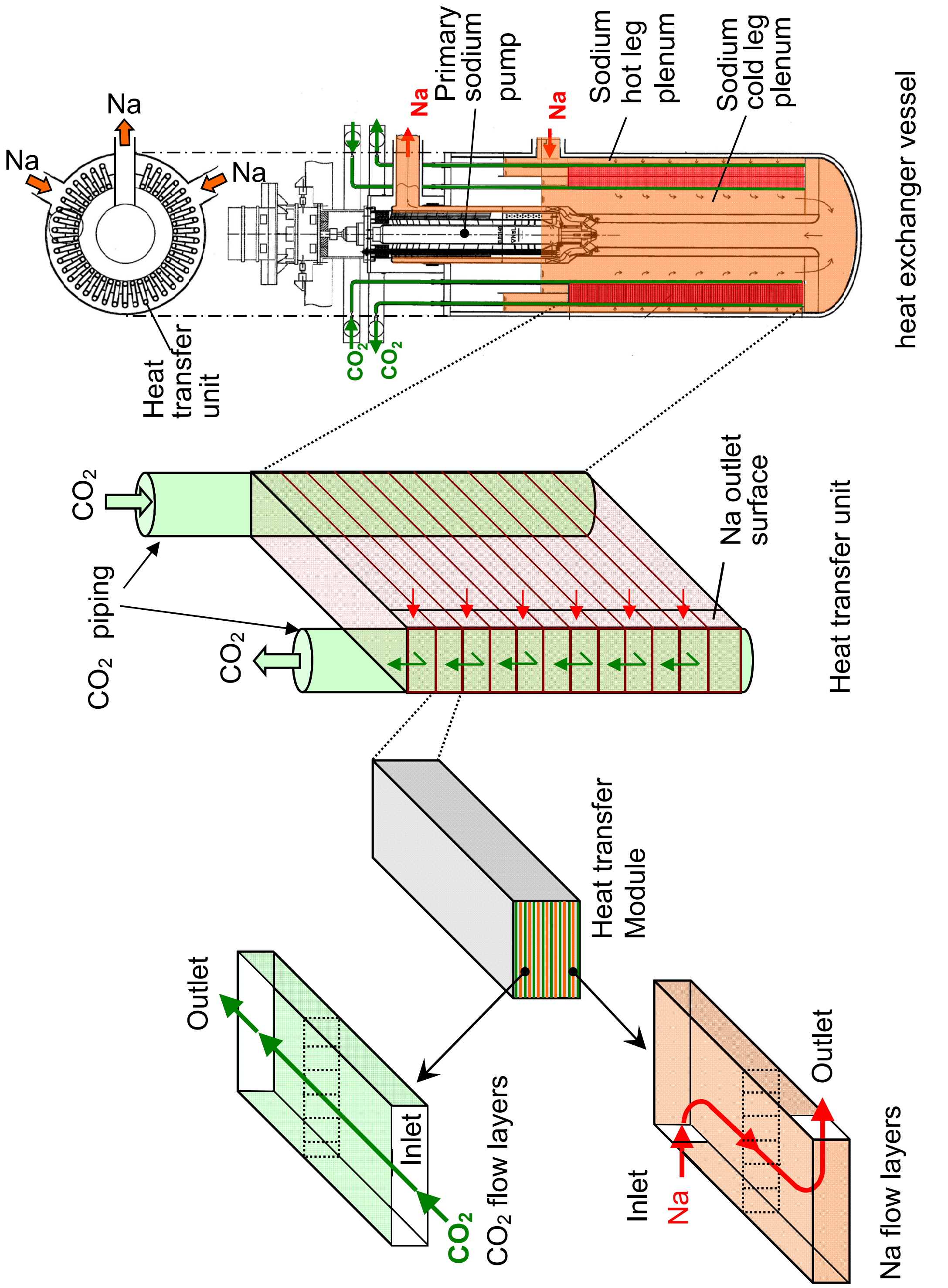

Fig. 3.3 Na/CO_2 heat exchanger

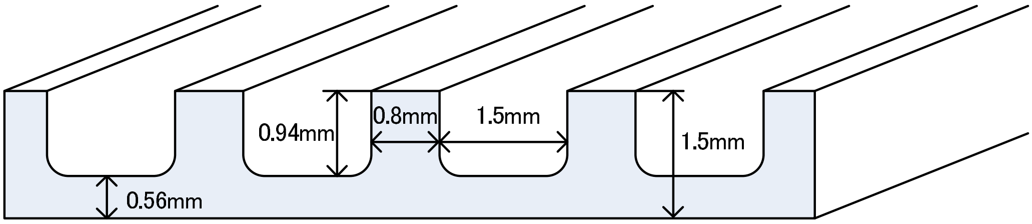

Item	Size
Plate thickness	1.5mm
Flow width	1.5mm
Flow path height	0.94mm
Fin thickness	0.8mm
Plate minimum thickness	0.56mm

Fig. 3.4 Na flow path of heat transfer module

Main specifications of heat transfer module

Dimensions	Width	230 mm
	Length	750 mm
	Height	202 mm
Heat transfer area		m^2
Heat transfer performance		817 kWth/Module
Pressure drop	Sodium side	0.017 MPa
	CO_2 side	0.242 MPa

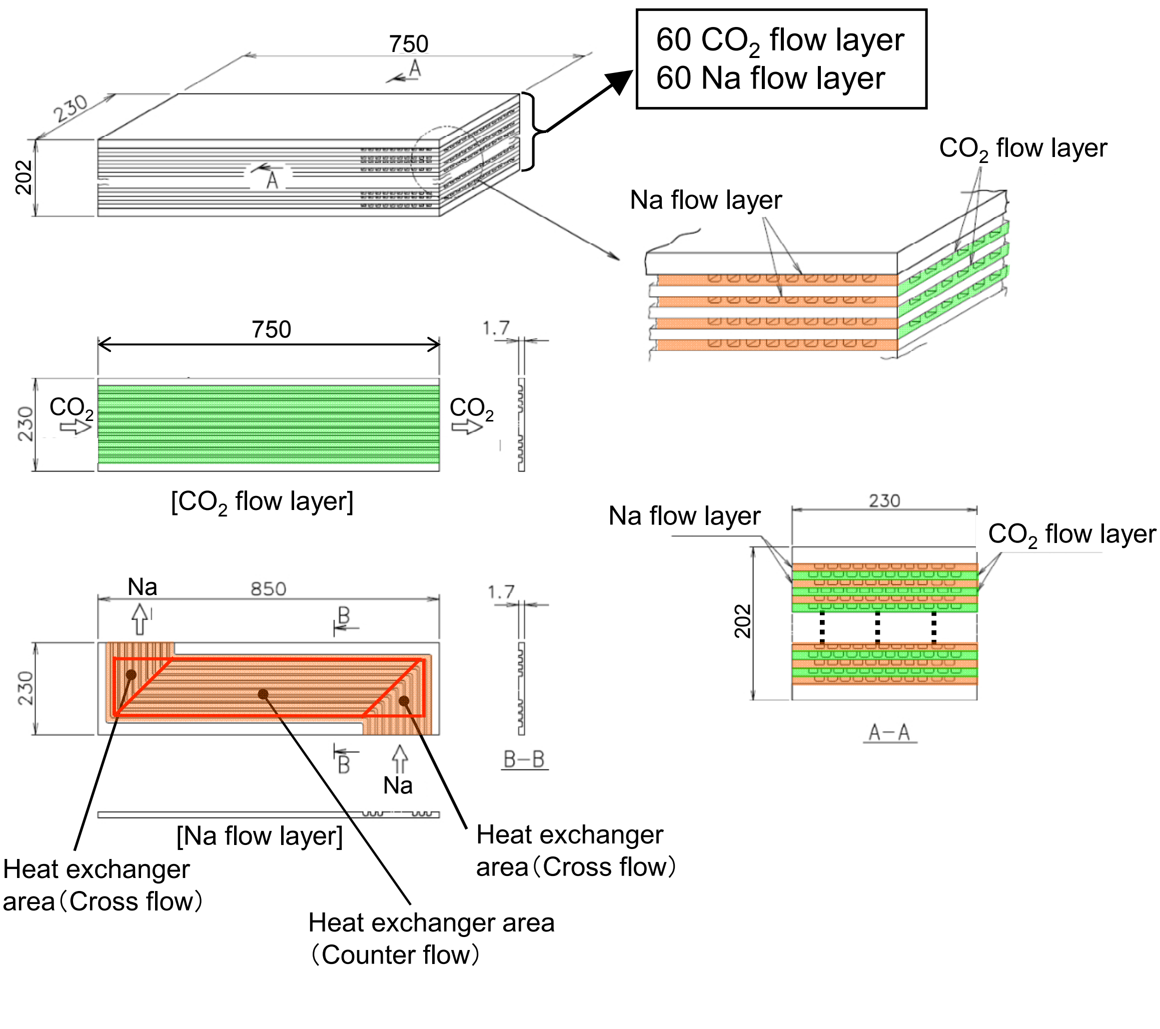

Fig. 3.5 Na/CO_2 heat transfer module

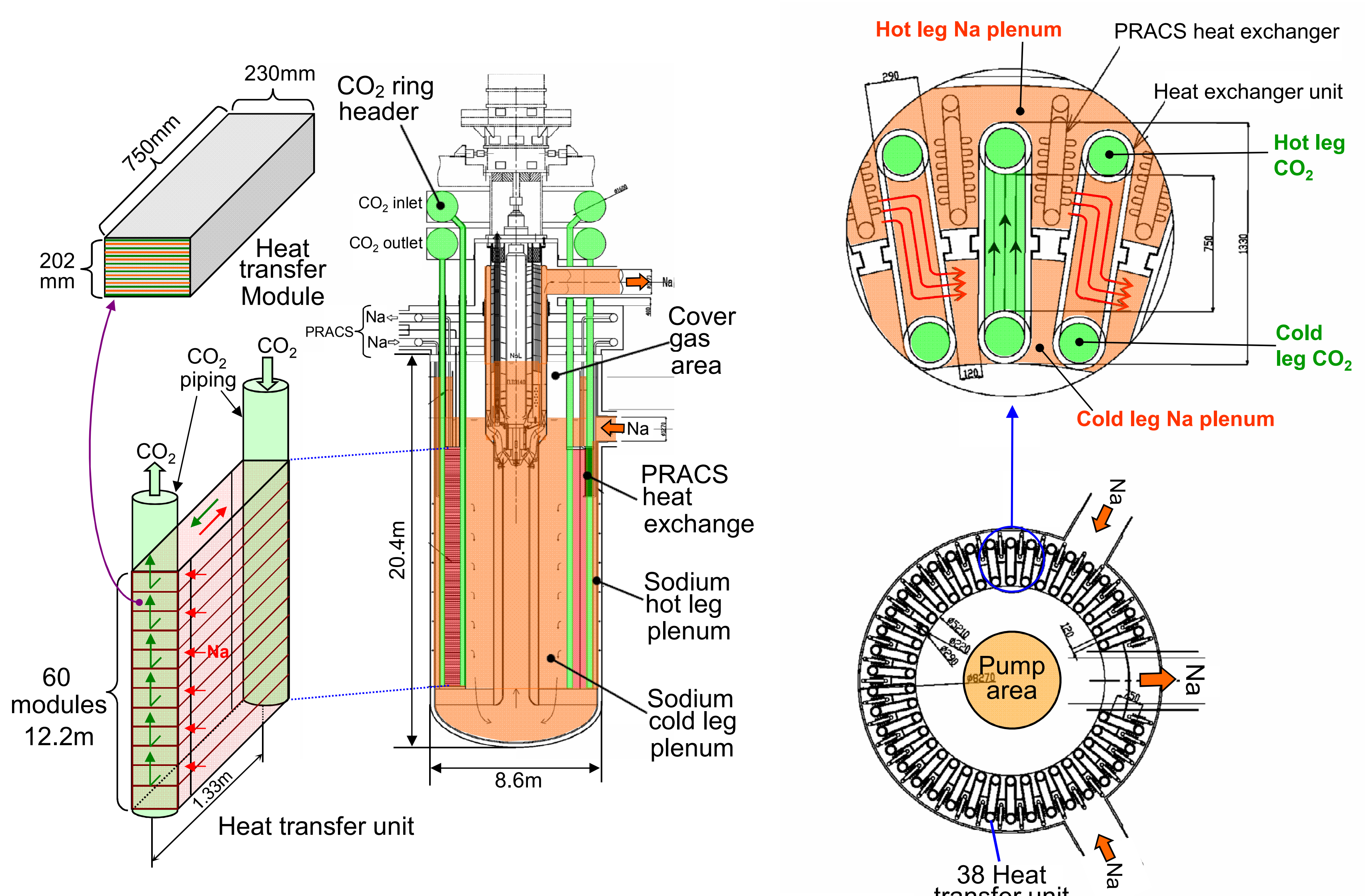

Fig. 3.6 Na/CO_2 heat exchanger

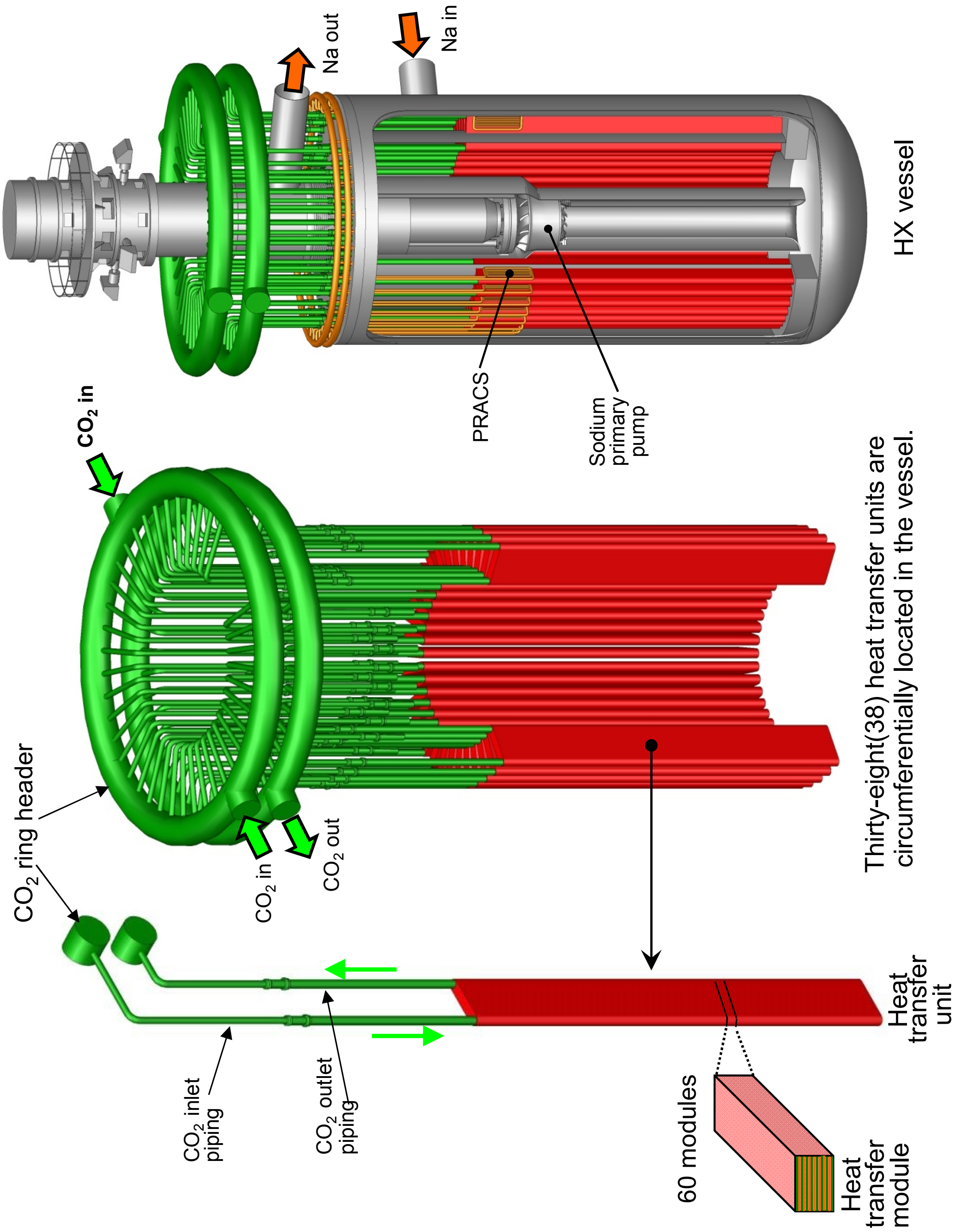

Fig. 3.7 3D view of Na/CO_2 heat exchanger

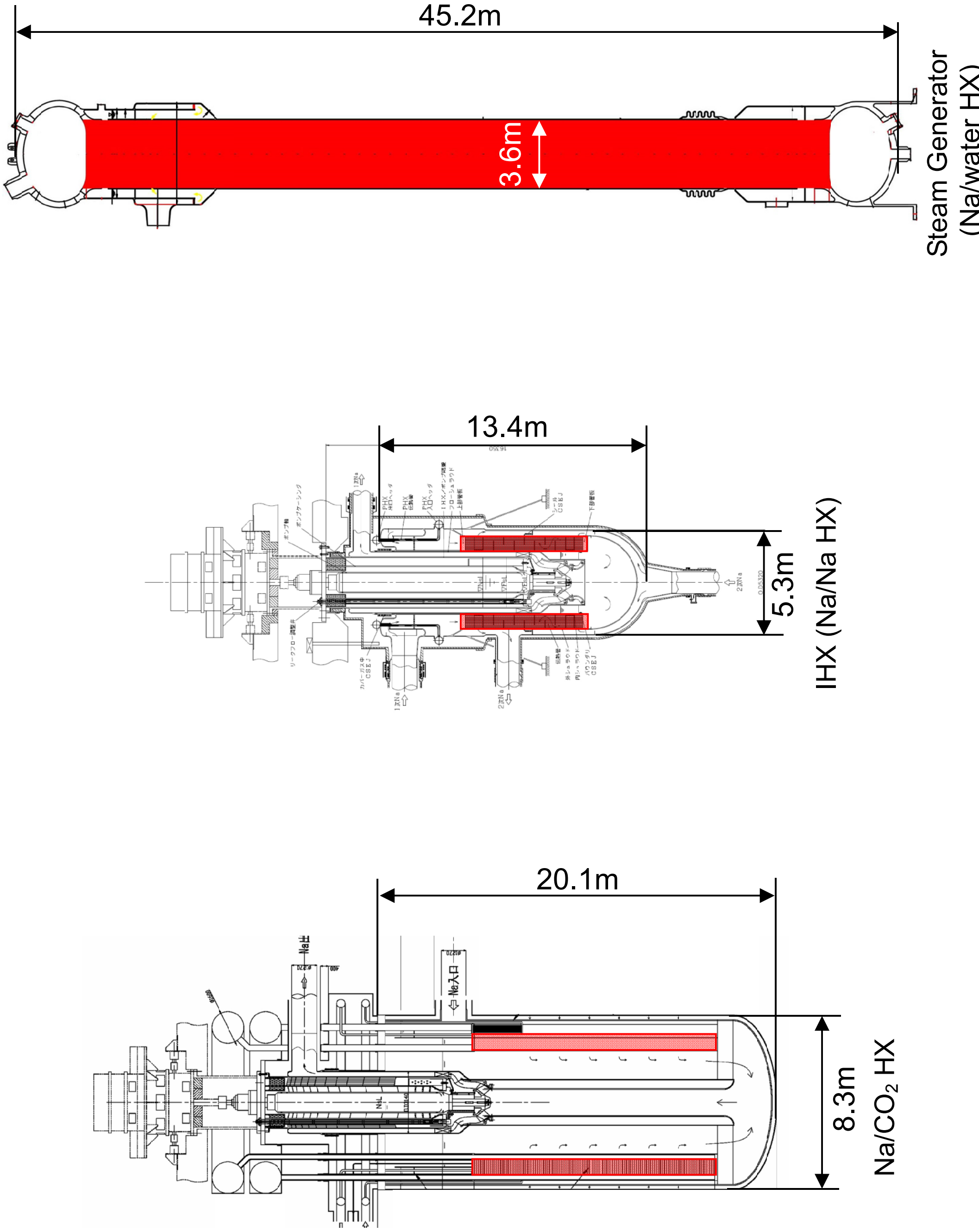

Fig. 3.8 Comparison between heat exchangers

4 Safety evaluation of Na/CO_2 reaction

4.1 Double-walled structure at Na/CO_2 boundary

The boundary between CO_2 and sodium exists in the PCHEs and along the CO_2 inlet/outlet piping. Providing a double-walled structure to these boundaries and continuous leak monitoring can prevent CO_2 leak into sodium.

It is impossible to inspect a heat transfer flow path in the PCHE due to access difficulty. Continuous CO_2 leak monitoring during plant operation was applied as an alternative to inspection.

4.1.1 Heat exchange region in heat exchanger unit

The PCHE module has a layered configuration of the SiC/SiC composite material plates, in which SiC fiber reinforced carbon layers are installed between sodium and CO_2-side flow paths, as is shown in Fig 4.1. The carbon layer was strengthened by the SiC fiber between SiC/SiC composite layers.

The leak detection grooves were horizontally arranged in the area surrounding the SiC fiber reinforced carbon layer as shown in Fig. 4.2. Leak detection holes vertically lead to these leak detection grooves of each layer. The leak detection holes were connected to the annulus of the double-walled CO_2 inlet/outlet piping.

Figure 4.3 shows a crack growth process from the CO_2 flow path in the PCHE. When a crack reaches the carbon layer, since the carbon layer is soft, the crack propagates horizontally in the carbon layer, not beyond the carbon layer. In this situation, the pressure of the CO_2 side (20 MPa) exerts on the carbon layer. However, since the carbon layer is firmly connected to the upper and lower SiC/SiC composite layers by the SiC fiber, no separation failure occurs between the carbon layers. The crack finally reaches the leak detection groove, to which CO_2 flows out. Since the leak detection grooves lead to the annulus of the CO_2 inlet/outlet piping through the leak detection holes, it is possible to detect CO_2 leaks by monitoring the gas in the annulus.

4.1.2 CO_2 inlet/outlet piping

The CO_2 inlet/outlet piping has a double-walled configuration consisting of inner and outer pipes. Filling the annulus between inner and outer pipes with inert gas and monitoring CO_2 concentration allow for detection of leaks at the stage of inner pipe failure, and thereby, prevent CO_2 leak into sodium.

4.2 Evaluation of Na/CO_2 reaction

4.2.1 Detection of CO_2 leak and mitigation of the effects

(1) CO_2 leak detection system

Assuming the case where CO_2 leaks into sodium regardless of the double-walled structure of the CO_2/sodium boundary, the monitoring of a CO_2 leak in sodium was studied.

The reaction between sodium and CO_2 is described as follows:

$$2Na + 2CO_2 = Na_2CO_3 + CO$$

This reaction equation indicates that CO and unreacted CO_2 exist in sodium in the form of gas. However, detection by means of permeation through nickel in sodium cannot be used for CO and CO_2, sampling cover gas method is effective.

(2) Effect mitigation system

A mitigation system is required to reduce the effects of a CO_2 leak into sodium. Leaked CO_2 needs to be separated from sodium to prevent the gas ingress into the reactor core. There are possible 3 places where the gas separator could be installed; inside the R/V, inside the heat exchanger vessel and at the outlet of the heat exchanger. The installation of a gas separator in the R/V requires a significant change in reactor structure. The installation of a gas separator at the heat exchanger outlet needs an additional vessel, increasing volume and occupied space. Therefore, the gas separation inside the heat exchanger vessel is suggested, and also a method of CO_2 release into the cover gas is desirable.

The ingress of CO_2 into sodium increases the pressure of the primary sodium system to above its allowance level. Accordingly, a pressure reducing equipment is also required and it needs to be connected to the cover gas region, to prevent sodium discharge during pressure relief process.

4.2.2 Safety evaluation for CO_2 leak

(1) CO_2 leak rate

In this heat exchanger, the boundary between CO_2 and sodium exists between the heat transfer flow paths of the PCHE modules and along the CO_2 inlet/outlet piping. Therefore, both regions have to be taken into account when assuming a failure in the Na/CO_2 boundary.

a) Failure in Na/CO_2 boundary between the heat transfer flow paths in PCHE

CO_2 flows out to the sodium side in the case of the Na/CO_2 boundary failure. The CO_2 pressure of approx. 20 MPa, causes a critical flow at a failure point. The pressure in the critical state depends on the pressure loss at a failure point; however, in this study, the critical pressure was assumed to be half the pressure on the CO_2 side, i.e., 10 MPa, for simple and conservative evaluation. The critical flow rate was calculated based on this assumption. The critical flow rate per unit cross section and the related information are listed in Table 4.1. This calculation also assumed that the conditions upstream from the failure point are the same as those at the CO_2 side outlet of the heat exchanger and that CO_2 adiabatically expands (isentropic change) when flowing out from the failure point.

The cross-section area of the sodium flow path of the PCHE is 1.41 mm^2, and the maximum CO_2 leak rate is determined by this cross-section area. The maximum leak rate was calculated from the cross-section area and Table 4.1 as follows:

$$4.23\times10^{-2}\ \mathrm{kg/sec} = 1.41\ \mathrm{mm^2} \times 3.0 \times 10^4\ \mathrm{kg/(m^2 \cdot sec)}$$

The flowing pattern is estimated that the sodium-side flow path is entirely filled with CO_2, as shown in Fig. 4.4. For conservative evaluation, the maximum CO_2 leak rate is assumed to be 5×10^{-2} kg/sec (50g/sec), somewhat larger than 4.23×10^{-2} kg/sec.

b) Failure in CO_2 inlet/outlet piping

CO_2 inlet/outlet piping failure causes much larger CO_2 leak rate than that of the flow path failure of a PHCE. Given an inner diameter of 36 mm (flow path cross-section area: 0.001 m^2), the leak rate is 60 kg/sec when assuming a double ended guillotine failure.

CO_2 leak events make various impacts, one of which is an increase in the cover gas(C/G) pressure. The limit of C/G pressure increase is set to be 0.1MPa to prevent the lifting of the reactor vessel rotating plug. However, the C/G pressure reaches the limit value within a few seconds after the CO_2 inlet/outlet piping failure. Since other effects are also significant, a double-walled structure was adopted for the CO_2 inlet/outlet piping to eliminate the possibility of the double ended guillotine failure.

(2) Effects of CO_2 leak

Na/CO_2 reaction accidents cause the reaction products, such as Na_2CO_3 and CO, change the pressure and flow conditions, giving effect on plant safety.

The basic requirements for ensuring plant safety include:

- reactor shutdown,
- decay heat removal, and
- radioactive material release mitigation.

Firstly, possible increase of the leak rate was examined, and then, the effects of and countermeasures for CO_2 leak events were studied from the above 3 safety requirements.

While the reaction between sodium and CO_2 depends on their mixing ratio, temperature, etc., the following reaction was assumed here:

$$Na(l) + CO_2\,(g) = 1/2Na_2CO_3(l) + 1/2CO(g)$$

Reaction heat [25°C] = 227 (kJ/mol)

Previous sodium/water reaction tests have revealed two mechanisms for the expansion of leak rate: wastage and over-heating rupture. In the case of a CO_2 leak, since the sodium flow path is a narrow region as shown in Fig. 4.4, there is no possibility that a large high-temperature reaction jet forms in the sodium side. Therefore, the expansion of failure due to over-heating rupture is unlikely. Wastage hardly advances the failure because the reaction products are Na_2CO_3, etc., which have low corrosiveness. And also, in-sodium CO_2 leak tests have shown that the amount of wastage was very small.

These facts indicate no significant escalation of CO_2 leak rate in the PCHE and not beyond the above-mentioned maximum CO_2 leak rate of approx. 50 g/sec.

a) Reactor shutdown

Three effects of CO_2 leak on reactor shutdown are as follows:

- Insertion of void reactivity by the effect of CO_2,

- Insertion of reactivity due to core compaction by pressure wave
- Hindering insertion of control rods due to core compaction by pressure wave

Since the CO_2 leak rate is not greater than 50 g/sec at maximum, as has already been described, the pressure wave generated in the PCHE is small and has no significant effect.

The insertion of void reactivity by gas was estimated by conservatively assuming that CO_2 does not decrease due to the reaction with sodium. The calculation conditions are as follows:

Maximum CO_2 leak rate: 50 g/sec
Mean core pressure: 0.3 MPa
Mean core temperature: 475℃
CO_2 density in the core: 2.2 kg/m^3
Coolant volume in the core: approx. 4.5 m^3
Core void reactivity: 5.2 \$ (1.14 \$/m^3)
Time needed for coolant to pass through the core: approx. 0.2 sec

The reactivity inserted at the maximum CO_2 leak rate was obtained based on these conditions. It was also assumed that CO_2 flows into the core from its bottom and is homogeneously distributed into the core with a certain void ratio within approximately 0.2 sec. This condition maximizes the reactivity.

Amount of CO_2 leak within 0.2 sec: 0.01 kg (= 0.05 kg/sec × 0.2 sec)
CO_2 volume: 0.0045 m^3 (= 0.01kg/2.2kg/m^3)
Inserted void reactivity: approx. 0.005 \$ (= 1.14 \$/m^3 × 0.0045 m^3)

The inserted reactivity was calculated to be approx. 0.005 \$. Even if a CO_2 leak cannot be detected before CO_2 reaches the core, the increase in reactor power due to the inserted reactivity is small.

The CO_2 leak rate corresponding to prompt criticality (1.0 \$) is 9.6 kg/sec (= ((1/1.14\$/m^3)×2.2 kg/m^3)/0.2 sec). A simultaneous failure of both the inner and outer CO_2 inlet/outlet pipes causes large CO_2 leak and then results in the prompt criticality. To avoid this event, the reactor core requires to be scrammed before the CO_2 gas reaches the core by detecting pressure increase.

b) Decay heat removal

A study was performed to investigate the possible effects of flow blockage (reduction in flow rate) due to reaction products and reduced heat transfer performance on decay heat removal.

The sodium inventory of the primary system is approx. 1000 tons (10^6 kg). Assuming that 1 kg of CO_2 leaking into the sodium system is entirely mixed into sodium and that no gaseous CO_2 is released into the cover gas region for conservative evaluation, the carbon and oxygen concentrations are increased by 0.27 ppm and 0.73 ppm, respectively. The upper limit of the oxygen concentration is 10 ppm and its concentration is ordinarily controlled from 3 to 5 ppm during normal operation. Provided that the total amount of the CO_2 leak is approx. 5 kg, it increases the oxygen and carbon concentrations by 5 ppm. This amount of the CO_2 causes no safety affects on the decay heat removal in the viewpoint of the impurity control. The 5 kg of CO_2 corresponds to the maximum leak rate of 50 g/sec for 100 seconds. If the 50 g/sec leak is detected in approx. 40 seconds and the CO_2 system is blown down in approx. 1 min., the amount of CO_2 leak can be restrained at an insignificant level.

c) Primary coolant boundary

For conservative estimation of the pressure increase in the primary system, leaked CO_2 was assumed not to be decreased by the reaction with sodium.

The total cover gas volume in the primary system is approx. 100 m^3 and the pressure increase of 0.1MPa at 400°C requires approx. 80 kg of CO_2. This corresponds to the amount of CO_2 leak rate of 50 g/sec for 1600 seconds. That is, as described above, the 40 sec. leak detection and the 1 min. CO_2 blow down can keep the pressure increase to no greater than 0.1 MPa.

To cope with beyond design basis accidents, such as the failure of the CO_2 inlet/outlet piping, it is necessary to take measures to mitigate the pressure increase by installing a rupture disk. The dump tank is possible spaces into which reaction products and CO_2 are released.

(3) Effect mitigation measures

In the Na/CO_2 heat exchanger, keeping the CO_2 leak rate less than approx. 50 g/sec limits the effect of Na/CO_2 boundary failure. Therefore, the requirement of the mitigation equipment can be reduced compared with the sodium heated steam generators.

The required measures are summarized as follows:

(i) Leak detection systems (gas chromatography in the cover gas, plugging indicator, cover gas pressure gauge)

(ii) Rapid CO_2 blow down system

(iii) Na/CO_2 reaction product release system (measure against BDBA)

(iv) RV-HX pressure equalizing line (measure to limit the transfer of reaction products from the hot leg, measure against BDBA)

Table 4.1 CO_2 critical flow rate

	HX outlet condition	Failure point
Pressure (MPa)	20	10
Temperature (℃)	527	450
Density (kg/m^3)	128	73
Entropy (kJ/(kg･K))	4.82	4.82
Velocity (m/s)	451	412
Critical flow rate (kg/(m^2･sec))	—	3.0×10^4

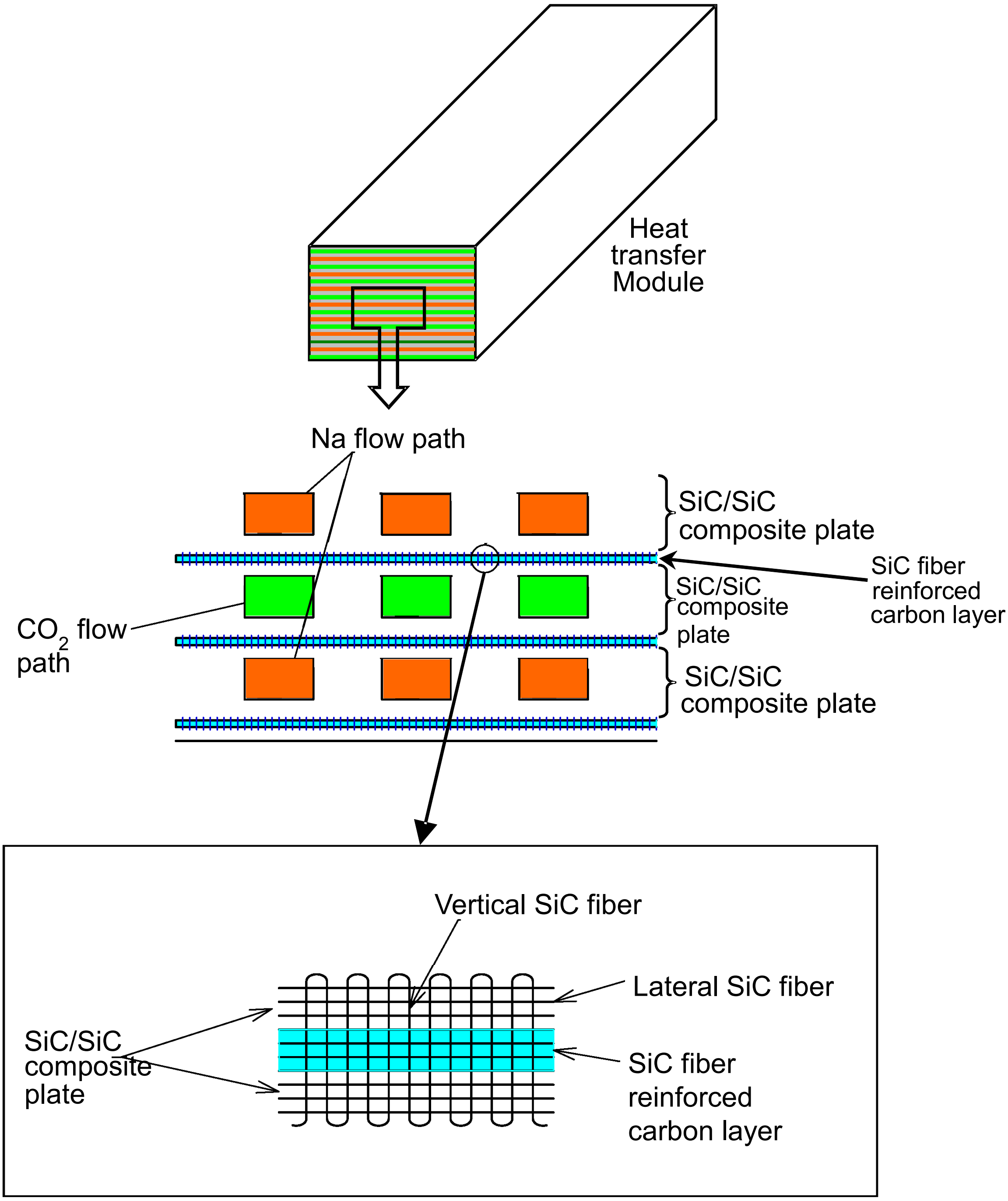

Fig. 4.1 Crack arresting of heat transfer module

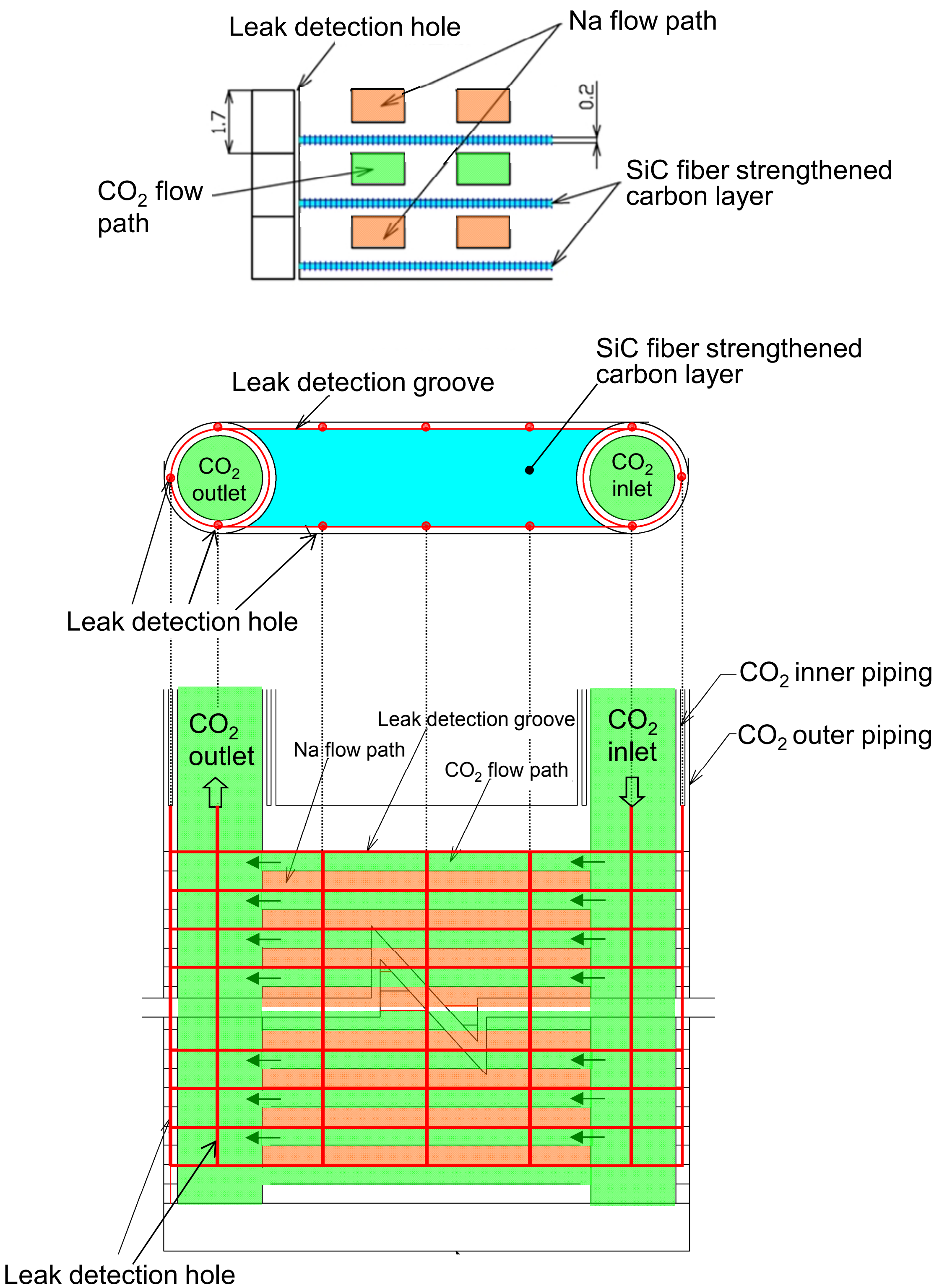

Fig. 4.2 Leak detection of heat transfer unit

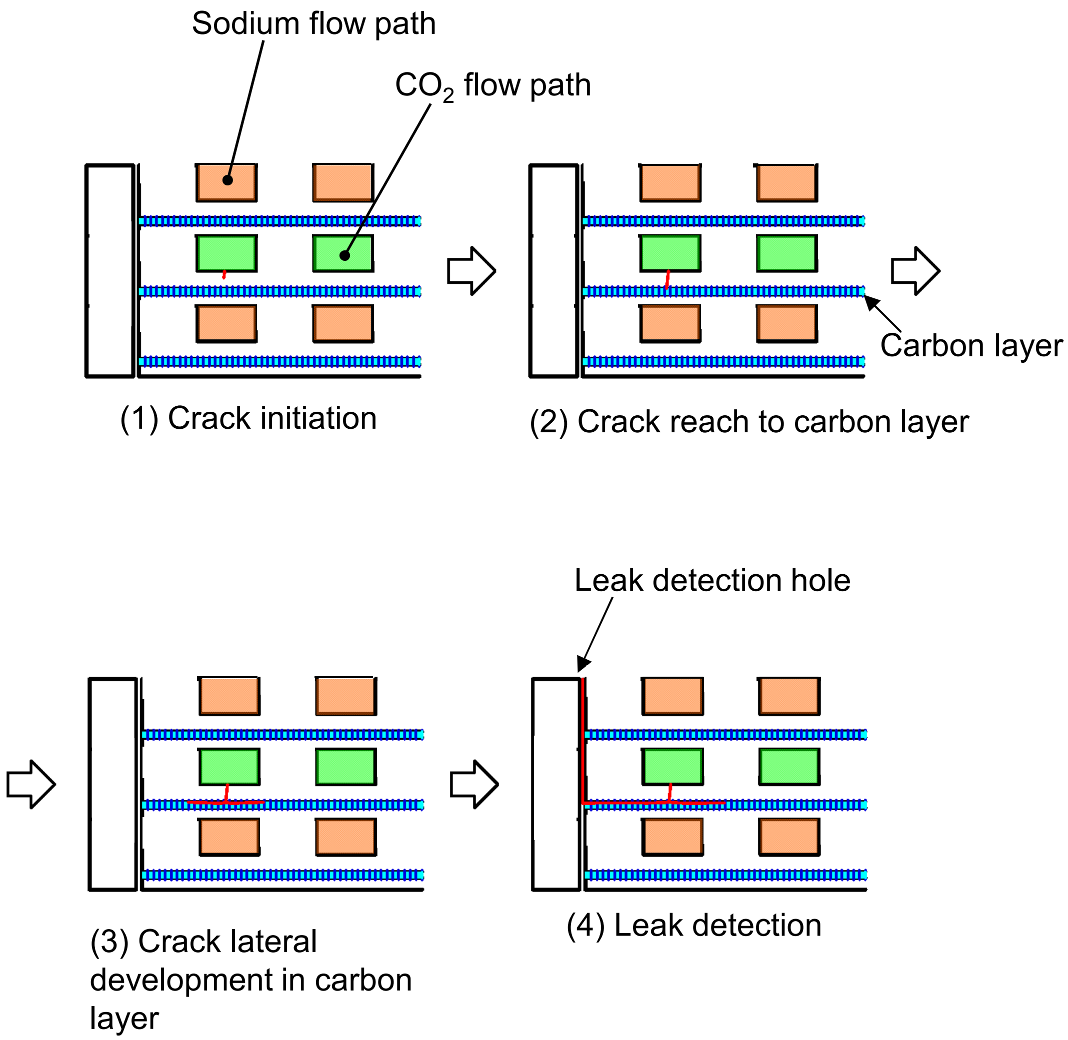

Fig. 4.3 Leak detection of heat transfer module

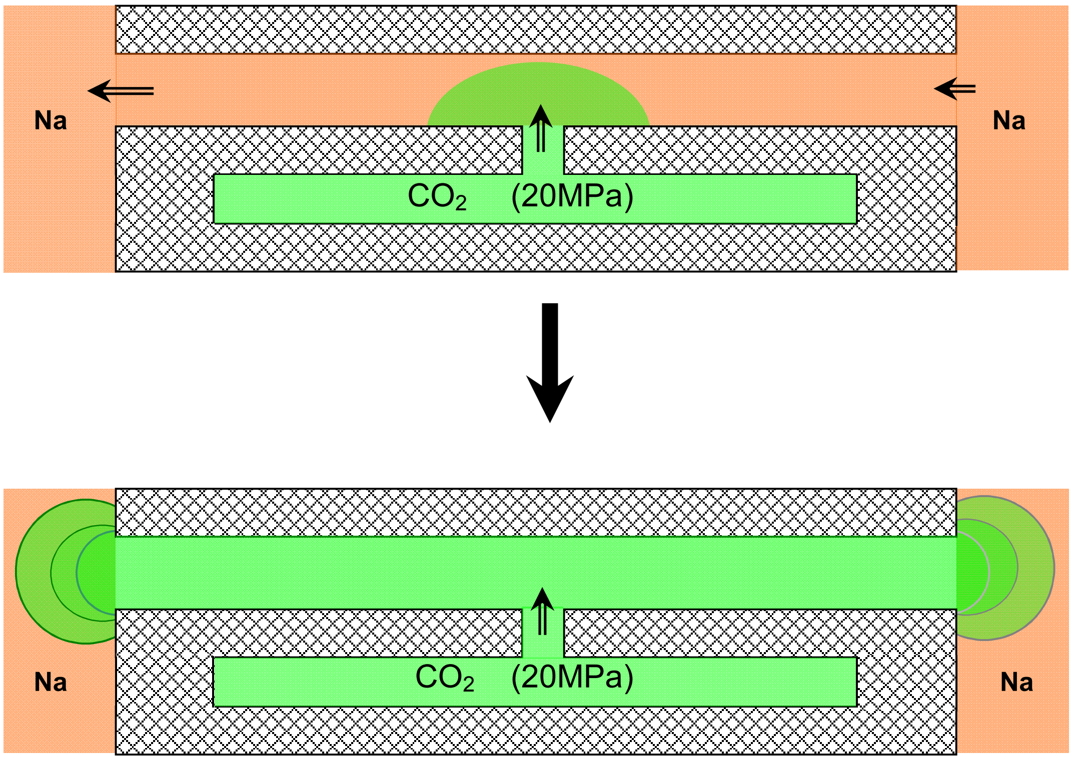

Fig. 4.4 CO_2 leak behavior in PCHE

5. Conclusions

The CO_2/Na reaction is not a furious event, and the area of failure in the PCHE is limited by its partitioned flow paths. Taking into account these advantages, a preliminary conceptual design of the secondary sodium circuit-eliminated JFSR adopting a supercritical CO_2 turbine system was performed.

The configuration of the Na/CO_2 heat exchanger was discussed in consideration of its heat transfer performance, safety, manufacturability, repairability. A simple evaluation of the effect of CO_2 leak on the reactor core and primary sodium boundary was also performed.

Since the PCHE has a large heat transfer area per unit volume, the volume of the heat transfer region is small. However, 38 PCHE modules are circumferentially arranged in the heat exchanger vessel to make space of the sodium and CO_2 flow paths, and this arrangement makes the vessel larger, compared with the IHX and SG.

No significant effect on the core and primary sodium boundary is caused by the CO_2 leak into sodium due to the failure of flow path in the PCHE because the leak flow rate and the area affected by failure are limited by the partitioned flow paths.

The layout of component/piping in the reactor building and the supercritical CO_2 gas turbine system (system configuration, heat and mass balance, layout, etc.) was also examined in the study of the secondary sodium circuit-eliminated JFSR. Based on these study results, the reduction in volume will be clarified by comparison with the reference JSFR (adopting the water-steam system with the secondary sodium circuit).

Acknowledgement

This design study was performed by the advice of Dr. Tatsuya HINOKI of Kyoto Univ., Dr. Yasushi MUTO and Dr. Takao ISHIZUKA of Tokyo Institute of Technology. Their advice was indispensable to accomplishing the study and is greatly appreciated.

References

(1) K. Aoto, N. Uto et al., "Design Study and R&D Progress on Japan Sodium-Cooled Fast Reactor," J. Nucl. Sci. Technol., Vol. 48, No. 4, 2011, pp.463-471.

(2) M. Aritomi, T. Ishizuka et al., "Performance Test Results of a Supercritical CO_2 Compressor Used in a New Gas Turbine Generating System," Journal of Power and Energy Systems, Vol. 5, No. 1, 2011, pp.45-59.

(3) Y. Muto and Y. Kato, "Design of Turbomachinery for the Supercritical CO_2 Gas Turbine Fast Reactor," Proc. of ICAPP'06, 6094 (2006).

(4) K. Nikitin, Y. Kato et al., "Experimental Thermal-hydraulics Comparison of Microchannel Heat Exchangers with Zigzag Channels and S-shaped Fins for Gas Turbine Reactors," Proc. of ICON15, 10826 (2007).

(5) T. Furukawa, Y. Inagaki et al., "Compatibility of FBR Structural Materials with Supercritical Carbon Dioxide," Progress in Nuclear Energy, 53, 2011, pp.1050-1055.

This is a blank page.

国際単位系（SI）

表１．SI 基本単位

基本量	SI 基本単位 名称	記号
長さ	メートル	m
質量	キログラム	kg
時間	秒	s
電流	アンペア	A
熱力学温度	ケルビン	K
物質量	モル	mol
光度	カンデラ	cd

表２．基本単位を用いて表されるSI組立単位の例

組立量	SI 基本単位 名称	記号
面積	平方メートル	m^2
体積	立法メートル	m^3
速さ，速度	メートル毎秒	m/s
加速度	メートル毎秒毎秒	m/s^2
波数	毎メートル	m^{-1}
密度，質量密度	キログラム毎立方メートル	kg/m^3
面積密度	キログラム毎平方メートル	kg/m^2
比体積	立方メートル毎キログラム	m^3/kg
電流密度	アンペア毎平方メートル	A/m^2
磁界の強さ	アンペア毎メートル	A/m
量濃度(a)，濃度	モル毎立方メートル	mol/m^3
質量濃度	キログラム毎立法メートル	kg/m^3
輝度	カンデラ毎平方メートル	cd/m^2
屈折率(b)	（数字の）　1	1
比透磁率(b)	（数字の）　1	1

（a）量濃度（amount concentration）は臨床化学の分野では物質濃度（substance concentration）ともよばれる。
（b）これらは無次元量あるいは次元１をもつ量であるが、そのことを表す単位記号である数字の１は通常は表記しない。

表３．固有の名称と記号で表されるSI組立単位

組立量	SI 組立単位 名称	記号	他のSI単位による表し方	SI基本単位による表し方
平面角	ラジアン(b)	rad	1 (b)	m/m
立体角	ステラジアン(b)	sr(c)	1 (b)	$m^{2/}m^2$
周波数	ヘルツ(d)	Hz		s^{-1}
力	ニュートン	N		$m\ kg\ s^{-2}$
圧力，応力	パスカル	Pa	N/m^2	$m^{-1}\ kg\ s^{-2}$
エネルギー，仕事，熱量	ジュール	J	N m	$m^2\ kg\ s^{-2}$
仕事率，工率，放射束	ワット	W	J/s	$m^2\ kg\ s^{-3}$
電荷，電気量	クーロン	C		s A
電位差（電圧），起電力	ボルト	V	W/A	$m^2\ kg\ s^{-3}\ A^{-1}$
静電容量	ファラド	F	C/V	$m^{-2}\ kg^{-1}\ s^4\ A^2$
電気抵抗	オーム	Ω	V/A	$m^2\ kg\ s^{-3}\ A^{-2}$
コンダクタンス	ジーメンス	S	A/V	$m^{-2}\ kg^{-1}\ s^3\ A^2$
磁束	ウエーバ	Wb	Vs	$m^2\ kg\ s^{-2}\ A^{-1}$
磁束密度	テスラ	T	Wb/m^2	$kg\ s^{-2}\ A^{-1}$
インダクタンス	ヘンリー	H	Wb/A	$m^2\ kg\ s^{-2}\ A^{-2}$
セルシウス温度	セルシウス度(e)	℃		K
光束	ルーメン	lm	cd sr(c)	cd
照度	ルクス	lx	lm/m^2	$m^{-2}\ cd$
放射性核種の放射能(f)	ベクレル(d)	Bq		s^{-1}
吸収線量, 比エネルギー分与, カーマ	グレイ	Gy	J/kg	$m^2\ s^{-2}$
線量当量, 周辺線量当量, 方向性線量当量, 個人線量当量	シーベルト(g)	Sv	J/kg	$m^2\ s^{-2}$
酸素活性	カタール	kat		$s^{-1}\ mol$

(a)SI接頭語は固有の名称と記号を持つ組立単位と組み合わせても使用できる。しかし接頭語を付した単位はもはやコヒーレントではない。
(b)ラジアンとステラジアンは数字の１に対する単位の特別な名称で、量についての情報をつたえるために使われる。実際には、使用する時には記号rad及びsrが用いられるが、習慣として組立単位としての記号である数字の１は明示されない。
(c)測光学ではステラジアンという名称と記号srを単位の表し方の中に、そのまま維持している。
(d)ヘルツは周期現象についてのみ、ベクレルは放射性核種の統計的過程についてのみ使用される。
(e)セルシウス度はケルビンの特別な名称で、セルシウス温度を表すために使用される。セルシウス度とケルビンの単位の大きさは同一である。したがって、温度差や温度間隔を表す数値はどちらの単位で表しても同じである。
(f)放射性核種の放射能（activity referred to a radionuclide）は、しばしば誤った用語で”radioactivity”と記される。
(g)単位シーベルト（PV,2002,70,205）についてはCIPM勧告2（CI-2002）を参照。

表４．単位の中に固有の名称と記号を含むSI組立単位の例

組立量	SI 組立単位 名称	記号	SI 基本単位による表し方
粘度	パスカル秒	Pa s	$m^{-1}\ kg\ s^{-1}$
力のモーメント	ニュートンメートル	N m	$m^2\ kg\ s^{-2}$
表面張力	ニュートン毎メートル	N/m	$kg\ s^{-2}$
角速度	ラジアン毎秒	rad/s	$m\ m^{-1}\ s^{-1}=s^{-1}$
角加速度	ラジアン毎秒毎秒	rad/s^2	$m\ m^{-1}\ s^{-2}=s^{-2}$
熱流密度，放射照度	ワット毎平方メートル	W/m^2	$kg\ s^{-3}$
熱容量，エントロピー	ジュール毎ケルビン	J/K	$m^2\ kg\ s^{-2}\ K^{-1}$
比熱容量，比エントロピー	ジュール毎キログラム毎ケルビン	J/(kg K)	$m^2\ s^{-2}\ K^{-1}$
比エネルギー	ジュール毎キログラム	J/kg	$m^2\ s^{-2}$
熱伝導率	ワット毎メートル毎ケルビン	W/(m K)	$m\ kg\ s^{-3}\ K^{-1}$
体積エネルギー	ジュール毎立方メートル	J/m^3	$m^{-1}\ kg\ s^{-2}$
電界の強さ	ボルト毎メートル	V/m	$m\ kg\ s^{-3}\ A^{-1}$
電荷密度	クーロン毎立方メートル	C/m^3	$m^{-3}\ sA$
表面電荷	クーロン毎平方メートル	C/m^2	$m^{-2}\ sA$
電束密度，電気変位	クーロン毎平方メートル	C/m^2	$m^{-2}\ sA$
誘電率	ファラド毎メートル	F/m	$m^{-3}\ kg^{-1}\ s^4\ A^2$
透磁率	ヘンリー毎メートル	H/m	$m\ kg\ s^{-2}\ A^{-2}$
モルエネルギー	ジュール毎モル	J/mol	$m^2\ kg\ s^{-2}\ mol^{-1}$
モルエントロピー, モル熱容量	ジュール毎モル毎ケルビン	J/(mol K)	$m^2\ kg\ s^{-2}\ K^{-1}\ mol^{-1}$
照射線量（Ｘ線及びγ線）	クーロン毎キログラム	C/kg	$kg^{-1}\ sA$
吸収線量率	グレイ毎秒	Gy/s	$m^2\ s^{-3}$
放射強度	ワット毎ステラジアン	W/sr	$m^4\ m^{-2}\ kg\ s^{-3}=m^2\ kg\ s^{-3}$
放射輝度	ワット毎平方メートル毎ステラジアン	$W/(m^2\ sr)$	$m^2\ m^{-2}\ kg\ s^{-3}=kg\ s^{-3}$
酵素活性濃度	カタール毎立方メートル	kat/m^3	$m^{-3}\ s^{-1}\ mol$

表５．SI 接頭語

乗数	接頭語	記号	乗数	接頭語	記号
10^{24}	ヨタ	Y	10^{-1}	デシ	d
10^{21}	ゼタ	Z	10^{-2}	センチ	c
10^{18}	エクサ	E	10^{-3}	ミリ	m
10^{15}	ペタ	P	10^{-6}	マイクロ	µ
10^{12}	テラ	T	10^{-9}	ナノ	n
10^9	ギガ	G	10^{-12}	ピコ	p
10^6	メガ	M	10^{-15}	フェムト	f
10^3	キロ	k	10^{-18}	アト	a
10^2	ヘクト	h	10^{-21}	ゼプト	z
10^1	デカ	da	10^{-24}	ヨクト	y

表６．SIに属さないが、SIと併用される単位

名称	記号	SI 単位による値
分	min	1 min=60s
時	h	1h =60 min=3600 s
日	d	1 d=24 h=86 400 s
度	°	1°=(π/180) rad
分	’	1’=(1/60)°=(π/10800) rad
秒	”	1”=(1/60)’=(π/648000) rad
ヘクタール	ha	$1ha=1hm^2=10^4m^2$
リットル	L，l	$1L=11=1dm^3=10^3cm^3=10^{-3}m^3$
トン	t	$1t=10^3$ kg

表７．SIに属さないが、SIと併用される単位で、SI単位で表される数値が実験的に得られるもの

名称	記号	SI 単位で表される数値
電子ボルト	eV	$1eV=1.602\ 176\ 53(14)\times10^{-19}J$
ダルトン	Da	$1Da=1.660\ 538\ 86(28)\times10^{-27}kg$
統一原子質量単位	u	1u=1 Da
天文単位	ua	$1ua=1.495\ 978\ 706\ 91(6)\times10^{11}m$

表８．SIに属さないが、SIと併用されるその他の単位

名称	記号	SI 単位で表される数値
バール	bar	$1\ bar=0.1MPa=100kPa=10^5Pa$
水銀柱ミリメートル	mmHg	1mmHg=133.322Pa
オングストローム	Å	$1\ Å=0.1nm=100pm=10^{-10}m$
海里	M	1 M=1852m
バーン	b	$1\ b=100fm^2=(10^{-12}cm)2=10^{-28}m^2$
ノット	kn	1 kn=(1852/3600)m/s
ネーパ	Np	SI単位との数値的な関係は、対数量の定義に依存。
ベル	B	
デジベル	dB	

表９．固有の名称をもつCGS組立単位

名称	記号	SI 単位で表される数値
エルグ	erg	$1\ erg=10^{-7}\ J$
ダイン	dyn	$1\ dyn=10^{-5}N$
ポアズ	P	$1\ P=1\ dyn\ s\ cm^{-2}=0.1Pa\ s$
ストークス	St	$1\ St\ =1cm^2\ s^{-1}=10^{-4}m^2\ s^{-1}$
スチルブ	sb	$1\ sb\ =1cd\ cm^{-2}=10^4cd\ m^{-2}$
フォト	ph	$1\ ph=1cd\ sr\ cm^{-2}\ 10^4lx$
ガル	Gal	$1\ Gal\ =1cm\ s^{-2}=10^{-2}ms^{-2}$
マクスウェル	Mx	$1\ Mx\ =\ 1G\ cm^2=10^{-8}Wb$
ガウス	G	$1\ G\ =1Mx\ cm^{-2}\ =10^{-4}T$
エルステッド(c)	Oe	$1\ Oe \triangleq (10^3/4π)A\ m^{-1}$

（c）３元系のCGS単位系とSIでは直接比較できないため、等号「 ≙ 」は対応関係を示すものである。

表10．SIに属さないその他の単位の例

名称	記号	SI 単位で表される数値
キュリー	Ci	$1\ Ci=3.7\times10^{10}Bq$
レントゲン	R	$1\ R = 2.58\times10^{-4}C/kg$
ラド	rad	$1\ rad=1cGy=10^{-2}Gy$
レム	rem	$1\ rem=1\ cSv=10^{-2}Sv$
ガンマ	γ	1 γ =1 nT=10-9T
フェルミ		1フェルミ=1 fm=10-15m
メートル系カラット		1メートル系カラット = 200 mg = 2×10-4kg
トル	Torr	1 Torr = (101 325/760) Pa
標準大気圧	atm	1 atm = 101 325 Pa
カロリー	cal	1cal=4.1858J（「15℃」カロリー），4.1868J（「IT」カロリー）4.184J（「熱化学」カロリー）
ミクロン	µ	$1\ µ\ =1µm=10^{-6}m$

（第8版，2006年改訂）